

Single Polymer Confinement in a Tube: Correlation between structure and dynamics

Joshua Kalb and Bulbul Chakraborty
*Martin Fisher School of Physics, Brandeis University,
 Mailstop 057, Waltham, Massachusetts 02454-9110, USA*
 (Dated: September 8, 2020)

Current work on biological systems and glass forming polymers has led to an interest in the study of confined polymer systems. The main questions concern the effects of confinement on the dynamics and the shape adopted by single polymers under hard and soft boundaries. In this paper, we construct an effective picture for the dynamics of an excluded-volume chain, under tube confinement, by combining scaling arguments for static correlation functions with a generalized Rouse model. The results are tested against Monte Carlo simulations using the bond-fluctuation algorithm, which uses a lattice representation of the polymer chain with excluded-volume effects.

INTRODUCTION

Confining polymers inevitably leads to a competition between internal cooperativity length scales and external geometry confining length scales. In polymers approaching the glass transition, relaxation takes place through cooperative rearrangement of monomers over large length scales; therefore, this competition should have particularly pronounced effects on the dynamics near the glass transition in thin polymer films[1, 2, 3]. In the realm of biological systems, macromolecules in a cell live in a crowded environment[4]. Besides the ubiquitous “excluded volume” effects arising from the large concentration of macromolecules inside cells, specific interactions and geometrical confinement impose constraints on the the dynamics of these molecules and affect cell functions. Recent studies of cellular transport, dynamical fluctuations of single enzymes, rheology of living cells and model biological systems indicate that crowded biological environments may give rise to glassy dynamics characterized by a broad distribution of timescales[5].

An important first step towards the understanding of confinement and crowding on the dynamics of polymers is the analysis of single-polymer-dynamics under geometrical confinement. The simplest example is that of a polymer confined to a tube. A scaling picture that has been useful for understanding the statics and dynamics of a single polymer in a tube is that of a succession of blobs with a radius equal to that of the tube. The size of the blob defines a screening length in the direction parallel to the tube beyond which excluded-volume interactions can be ignored[6, 7]. To our knowledge, there is no extension of the blob-picture based calculations of dynamical correlations to confinement in higher dimensions. There is, however, a generalized blob picture for calculating static correlation functions in higher dimensions[8].

The main subject of this paper is the construction of a framework for calculating dynamical correlation functions for polymers under confinement that is not limited to the tube geometry. In the first half of the paper, we discuss static correlation functions for a polymer confined to a tube and compare the results of the blob picture to

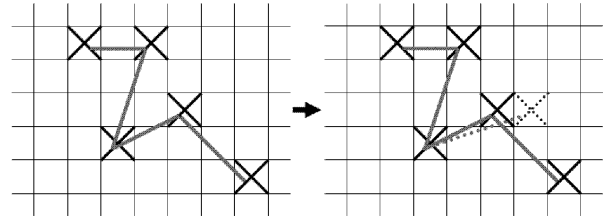


FIG. 1: Potential move for the bond-fluctuation model. Each monomer occupies one box and bonds are drawn in grey. The magnitude of the bond vector \mathbf{v} is $2 < |\mathbf{v}| < 13$ for the 2-D bond-fluctuation model

Monte Carlo simulations. In the second half, we write down a generalized Rouse model for the dynamics which includes the effects of confinement and excluded-volume by exploiting the blob-scaling results for static correlations. The predictions of this dynamical model are compared to simulation results for a polymer confined to a tube.

The simulations are based on the bond fluctuation algorithm, a lattice-based algorithm that allows for the analysis of dynamical properties of polymers[9]. As the name implies, the algorithm allows for fluctuations of bond lengths and employs only local moves of monomers. Excluded-volume effects are taken into account by ensuring the initial polymer configuration contains no intersecting bonds and by allowing only the following set of bonds:

$$S = (2, 0) \cup (2, 1) \cup (2, 2) \cup (3, 0) \cup (3, 1) \cup (3, 2)$$

This also leads to an effective monomer size b , where $b \approx 2.8$ lattice spacings.

The simulated dynamics reproduces generalized Rouse dynamics for excluded-volume polymers[10] in all spatial dimensions, and the algorithm has been widely used to study the dynamics in different environments[11, 12, 13, 14]. Our aim is to construct a course-grained picture of the dynamics of a polymer in a tube. The simulation results will be used as a support for the derivations from the blob picture.

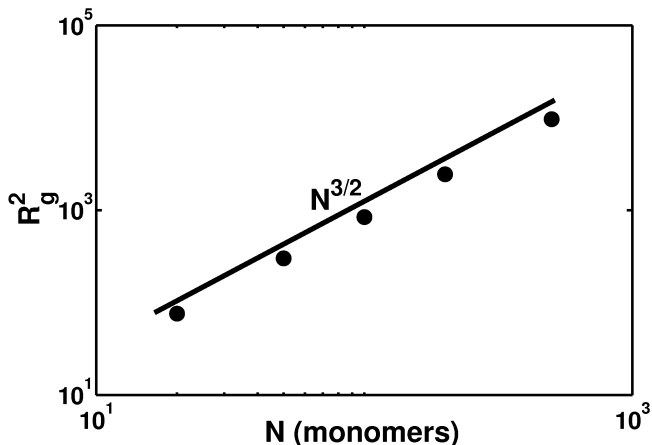


FIG. 2: Radius of gyration squared versus monomer number taken from simulation data. All length scales are in terms of lattice spaces.

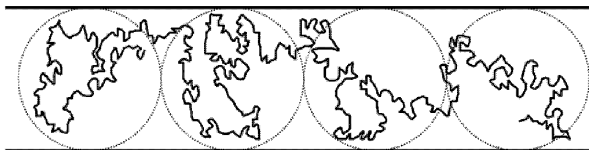


FIG. 3: Sample configuration from simulation of a 2-D polymer confined to a tube. Circles indicate rough shape of the blobs.

SHAPE OF A POLYMER IN A TUBE

For an unconfined polymer, consisting of N monomers of size b , the radius of gyration is given by[15]:

$$R_g \sim bN^\nu$$

$$\nu = \frac{3}{d+2} \quad (1)$$

where ν is the Flory exponent[16] and d is the spatial dimension. (For the simulations, b and other quantities of length will be expressed in terms of lattice spacings.)

This expression for ν is exact in $d = 2$ and $d = 4$. For $d = 3$, it differs from the measured value by about 1% ($\nu \sim 0.588$). For $d > 4$, excluded volume effects become irrelevant and $\nu = 1/2$ [17].

Upon confining this self-avoiding walk (SAW) to a tube, we expect the excluded volume effects to change the overall shape of the polymer. We now review the blob picture and then compare its predictions to the simulation results.

blob Picture In a tube of width $L < R_g$, where R_g is the radius of gyration of the free polymer, confinement has the effect of stretching the polymer in the axial direction and screening out the excluded volume interactions beyond a length scale comparable to L . The polymer can be visualized as a succession of blobs with excluded-volume effects being maintained for distances smaller

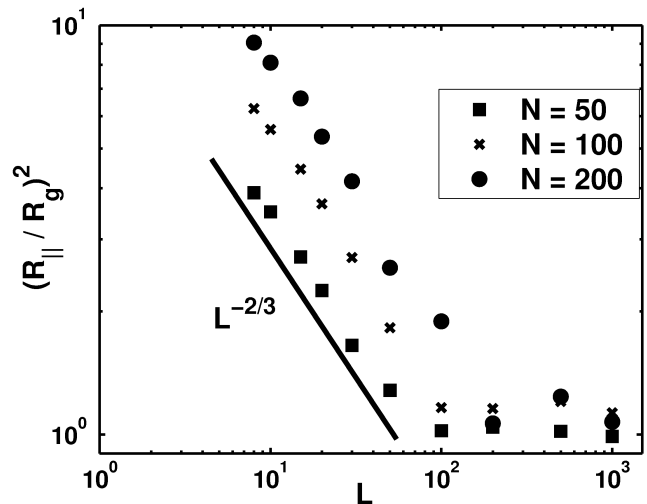


FIG. 4: $(R_{||}/R_g)^2$ versus tube width for varying polymer lengths, N

than the blob size[7]. The number, g , of monomers per blob can be calculated by requiring that the radius of gyration of these monomers matches the confinement length scale[14]. For the tube geometry, the radius of gyration of the blob is L and,

$$L \sim bg^\nu$$

$$g \sim \left(\frac{L}{b}\right)^{1/\nu} \quad (2)$$

The polymer is composed of N_b blobs and has a lateral extension of:

$$R_{||} \sim LN_b \quad (3)$$

Since the number of monomers is fixed at N ,

$$N = gN_b \Rightarrow N_b = \frac{N}{g} \quad (4)$$

Combining Eq.(2), (3), and (4), the magnitude of the parallel component of the average end-to-end vector for a 2-D polymer confined to a tube of width L is[18]

$$R_{||} \sim Nb \left(\frac{b}{L}\right)^{1/\nu-1} \sim Nb \left(\frac{b}{L}\right)^{1/3} \quad (5)$$

We support this scaling with simulation results (see Fig.4). In addition, since the tube width confines the polymer in the perpendicular direction[19]:

$$R_{\perp} \sim L \quad (6)$$

as shown in Fig.5.

Monomer-Monomer correlation function The previous argument holds for the end-to-end vector scaling, but we could just have easily considered any two points on the

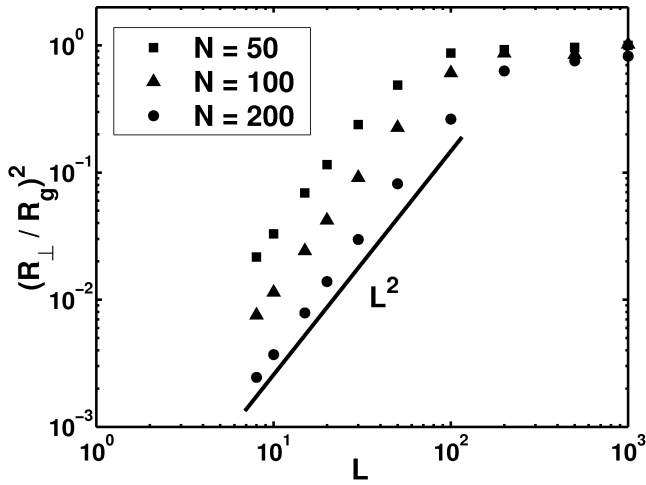


FIG. 5: $(R_{\perp}/R_g)^2$ versus tube width for varying polymer lengths, N

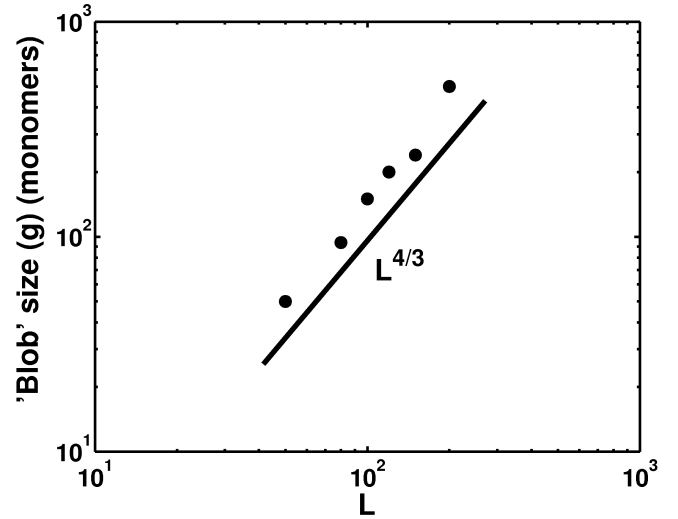


FIG. 7: Effective number of monomer per blob, g , in terms of box for $N = 10000$.

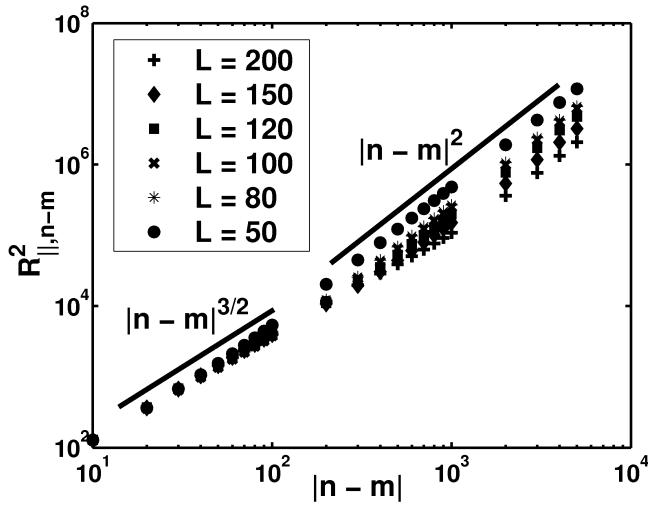


FIG. 6: Values of $R_{||,n-m}$ for $N = 10000$ as a function of separation along the chain, $n - m$, for various L , where $L < R_g$. Crossover to rigid-rod scaling occurs at larger monomer separations along the chain with larger L .

chain. This would imply that the free chain scaling holds for the 2-D self-avoiding walk so long as the sub-chains we consider are smaller than the blob size. Therefore, we expect the following behavior to hold generally for 2-D chains confined to a tube of width L :

$$R_{||,n-m}^2 \sim \begin{cases} |n-m|^{3/2} b^2 & |n-m| < (\frac{L}{b})^{4/3} \\ |n-m|^2 b^{8/3} L^{-2/3} & |n-m| > (\frac{L}{b})^{4/3} \end{cases} \quad (7)$$

$$R_{\perp,n-m}^2 \sim \begin{cases} |n-m|^{3/2} b^2 & |n-m| < (\frac{L}{b})^{4/3} \\ L^2 & |n-m| > (\frac{L}{b})^{4/3} \end{cases} \quad (8)$$

where

$$R_{||,n-m}^2 = \langle (x_{n||} - x_{m||})^2 \rangle \quad (9)$$

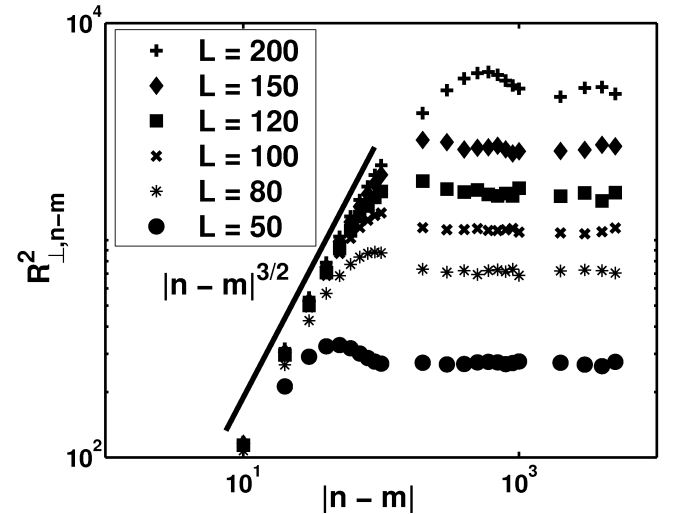


FIG. 8: Values of $R_{\perp,n-m}$ for $N = 10000$ as a function of separation along the chain, $n - m$, for various L , where $L < R_g$. Crossover to a saturation value occurs at larger monomer separations along the chain with larger L .

and

$$R_{\perp,n-m}^2 = \langle (x_{n\perp} - x_{m\perp})^2 \rangle \quad (10)$$

For a consistency check, we note that the chain scaling is that for a free polymer throughout the whole chain for $L \sim R_g$. In the perpendicular direction, the damped oscillatory behavior persists even after the saturation value due to the finite chain length. The parallel scaling is particularly interesting. The long chain correlations correspond to rigid-rod scaling as expected for a self-avoiding walk in 1-D.

Simulations results for these correlation functions are compared to the predictions in Fig.6 and 8. Fig.6 demon-

strates the change in scaling of $R_{||,n-m}^2$ with increasing distance between monomers. The size of the chain, $N = 10000$, was chosen to best illustrate the blobs. The blob size shows up in Fig.6 and 8 as the length scale at which the monomer-monomer changes and can be plotted explicitly (see Fig.7). The simulations thus support the scaling results emerging from the blob picture. In the following section, we investigate the dynamics

DYNAMICS

Unconfined polymer

Early time behavior of a polymer can be described using well known scaling arguments[10]. Through dimensional analysis:

$$\langle (\mathbf{r}_n(\mathbf{t}) - \mathbf{r}_n(\mathbf{0}))^2 \rangle \sim R_g^2 f \left(\frac{k_B T t}{\zeta R_g^2}, N \right) \quad (11)$$

where $\mathbf{r}_n(\mathbf{t})$ is the position of the n^{th} monomer along the chain at time \mathbf{t} , ζ is the drag coefficient of the medium in which the polymer, k_B is Boltzmann's constant, and T is temperature.

We have two additional pieces of information:(i) the chain size is fixed under renormalization of the monomer size and chain length, (ii) at short times, the monomer has not interacted with the whole chain so the dynamics should be independent of N . From the first assumption,

$$\langle (\mathbf{x}_n(\mathbf{t}) - \mathbf{x}_n(\mathbf{0}))^2 \rangle \sim R_g^2 f \left(\frac{k_B T t}{\zeta N R_g^2} \right) \quad (12)$$

and from the second

$$\begin{aligned} \langle (\mathbf{x}_n(\mathbf{t}) - \mathbf{x}_n(\mathbf{0}))^2 \rangle &\sim b^2 N^{3/2} \left(\frac{k_B T t}{\zeta N^{5/2} b^2} \right)^a \\ &\sim N^0 \end{aligned} \quad (13)$$

which implies

$$\langle (\mathbf{x}_n(\mathbf{t}) - \mathbf{x}_n(\mathbf{0}))^2 \rangle \sim t^{3/5} \quad (14)$$

This behavior holds up to the rotational relaxation time

$$\tau \sim \frac{\zeta b^2 N^{5/2}}{k_B T} \quad (15)$$

at which point the system crosses over to purely diffusive behavior

$$\langle (\mathbf{x}_n(\mathbf{t}) - \mathbf{x}_n(\mathbf{0}))^2 \rangle \sim \frac{k_B T t}{\zeta N b^2} \quad (16)$$

Rouse modes The dynamics of a polymer in tube have been worked out in the past using scaling arguments. Here we present a derivation that arrives at a similar result using the equi-partition theorem.

To derive the dynamics, we write down the sum of all the forces acting on a particular bead for an ideal unconfined chain[10, 16].

$$\zeta \frac{\partial \mathbf{x}_n}{\partial t} = k(\mathbf{x}_{n+1} - 2\mathbf{x}_n + \mathbf{x}_{n-1}) + \mathbf{g}_n(\mathbf{t}) \quad (17)$$

where $\mathbf{g}(\mathbf{t})$ is a random force on each bead and

$$k = \frac{k_B T}{b^2} \quad (18)$$

If we are considering dynamics at length scales much greater than the individual monomer spacing, b , we can rewrite Eq.(17) as

$$\zeta \frac{\partial \mathbf{x}}{\partial t} = k \frac{\partial^2 \mathbf{x}}{\partial n^2} + \mathbf{g}(\mathbf{x}, \mathbf{t}) \quad (19)$$

$$\langle \mathbf{g}_j(\mathbf{x}, \mathbf{t}) \rangle = \mathbf{0} \quad (20)$$

$$\langle \mathbf{g}_j(\mathbf{x}, \mathbf{t}) \mathbf{g}_k(\mathbf{x}', \mathbf{t}') \rangle = \frac{k_B T}{N} \delta_{jk} \delta(\mathbf{t} - \mathbf{t}') \delta(\mathbf{x} - \mathbf{x}') \quad (21)$$

where j and k are the cartesian components of $\mathbf{g}(\mathbf{x}, \mathbf{t})$.

Upon Fourier transforming this equation in n -space, we arrive at the equation for the Rouse modes.

$$\zeta_p \frac{\partial \mathbf{X}_{pj}}{\partial t} = -k_{pj} \mathbf{X}_{pj} + \mathbf{g}_{pj}(\mathbf{t}) \quad (22)$$

with

$$\zeta_p = N \zeta \quad (23)$$

and

$$k_{pj} \sim \frac{p^2}{N b^2} \quad (24)$$

The modes are defined by[10]:

$$\mathbf{X}_{pj} = \frac{1}{N} \int_0^N dn \cos \left(\frac{p\pi n}{N} \right) \mathbf{x}_{nj}(t) \quad (25)$$

or

$$\mathbf{X}_{pj} = -\frac{1}{p\pi} \int_0^N dn \sin \left(\frac{p\pi n}{N} \right) \frac{\partial \mathbf{x}_{nj}(t)}{\partial n} \quad (26)$$

Eq.(22) is a linear Langevin equation and can be solved exactly.

For a chain with self-avoidance, we write the Langevin equation including the self-avoidance interaction term, \mathbf{f}_{SA} .

$$\zeta \frac{\partial \mathbf{x}_n}{\partial t} = k(\mathbf{x}_{n+1} - 2\mathbf{x}_n + \mathbf{x}_{n-1}) + \mathbf{f}_{SA} + \mathbf{g}_n(\mathbf{t}) \quad (27)$$

Normally, this type of equation has no analytic solution. However, if coupling between normal modes is neglected, we arrive at an effective linear equation[10, 20].

$$\zeta_p \frac{\partial \mathbf{X}_{pj}}{\partial t} = -k_{pj} \mathbf{X}_{pj} + \mathbf{g}_{pj}(\mathbf{t}) \quad (28)$$

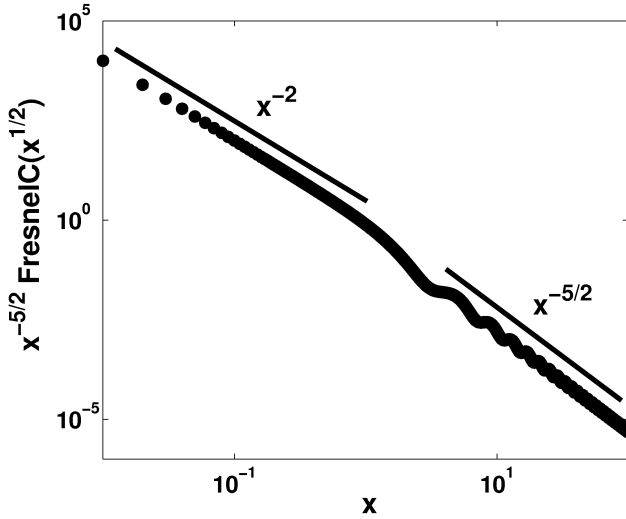


FIG. 9: Example behavior of $x^{-5/2}F_C(x^{1/2})$ as a function of various mode numbers where $x \sim (p(L/b)^{4/3}/N)$. This would imply that large x corresponds to short modes and the small x to long modes.

All the self-avoidance and boundary effects are incorporated through the k_{pj} term. In the long time limit, the equi-partition theorem applies[16] and we have the relation:

$$k_{pj} \sim \frac{k_B T}{\langle X_{pj}^2 \rangle_{eq}} \quad (29)$$

where $\langle \cdot \rangle_{eq}$ implies an equilibrium average. Using the methods of Doi and Edwards[16], we then express $\langle X_{pj}^2 \rangle_{eq}$ in terms of the static correlation functions:

$$\langle X_{pj}^2 \rangle_{eq} \sim \frac{N}{p^2} \int_0^N du \cos\left(\frac{p\pi u}{N}\right) \times \frac{\partial^2 \langle (x_{mj} - x_{nj})^2 \rangle_{eq}}{\partial n \partial m} \quad (30)$$

where $u = m - n$ and $p \gg 1$.

This result implies that given a second moment of the equilibrium distribution values we can recover the modes and ultimately the dynamics.

Confined Polymer

For a polymer confined to a tube, the form of $\langle (x_{mj} - x_{nj})^2 \rangle$ is predicted by the blob picture from the previous section on equilibrium behavior. We will use this result to extract the dynamical behavior.

Transverse Motion To study the system effectively, we break up the modes into directions perpendicular to the walls, $X_{p\perp}$, and parallel to the walls, $X_{p\parallel}$. For $p \geq N/g$:

$$\begin{aligned} \langle X_{p\perp}^2 \rangle_{eq} &\sim \frac{N}{p^2} \int_0^g du \cos\left(\frac{p\pi u}{N}\right) \times \frac{\partial^2 \langle (x_{m\perp} - x_{n\perp})^2 \rangle_{eq}}{\partial n \partial m} \\ &\sim \frac{N}{p^2} \int_0^{(L/b)^{4/3}} du \cos\left(\frac{p\pi u}{N}\right) \frac{1}{u^{1/2}} \\ &\sim \frac{N^{3/2} b^2}{p^{5/2}} F_c\left(\frac{2^{1/2} p^{1/2} L^{2/3}}{N^{1/2} b^{2/3}}\right) \end{aligned} \quad (31)$$

$F_c(\cdot)$ is the Fresnel Cosine function which can be approximated as a linear function of the argument for small arguments and constant for large arguments (See Fig.9).

Since we know the definition of a mode in terms of the monomer positions, we can invert this relation to predict dynamical quantities in the system such as individual monomer motion, center of mass motion, and two time correlation functions.

The form of the modes perpendicular to the walls will be the same as the unconfined chain modes. However, the hard boundary walls serve as a cutoff to the modes which implies that there exists a longest mode. Physically this would correspond to a smallest finite p for the perpendicular direction. Since u/N would correspond to the fraction of monomers inside a blob, p corresponds to $1/(\text{fractions of monomers inside a blob})$. This corresponds to g/N of the monomers moving at once or a longest mode of $p = N/g$. Starting from Eq.(26) and making use of the fact there is a longest mode, it can be shown that:

$$\langle (x_{n\perp}(t) - x_{n\perp}(0))^2 \rangle = \frac{L^2}{N} \left[1 - \exp\left(-\frac{tb^{4/3}}{L^{10/3}}\right) \right] + 4 \sum_{p=1}^{\infty} \cos^2\left(\frac{p\pi n}{N}\right) \frac{1}{k_{p\perp}} \left[1 - \exp\left(-\frac{t}{\tau_{p\perp}}\right) \right] \quad (32)$$

where

$$\tau_{p\perp} = \frac{\zeta_p}{k_{p\perp}} \sim \frac{N\zeta \langle X_{p\perp}^2 \rangle_{eq}}{k_B T} \quad (33)$$

The first term in Eq.(32) is the 0^{th} mode and associated with the center-of-mass motion, the longest time behavior. It tells us that perpendicular to the walls, the center of mass reaches a saturation value dependent on

the polymer size and tube width. However, the time at which the crossover occurs is independent of the polymer length implying only a dependence on the blob size. For early times, the sum needs to be taken into account.

$$\langle (x_{n\perp}(t) - x_{n\perp}(0))^2 \rangle \sim \int_{N/g}^{\infty} dp \frac{1}{k_{p\perp}} \left[1 - \exp\left(-\frac{t}{\tau_{p\perp}}\right) \right] = L^2 \left[1 - \exp\left(-\frac{tb^{4/3}}{L^{10/3}}\right) \right] + b^2 t^{3/5} \Gamma_{tb^{4/3}/L^{10/3}} \left(\frac{2}{5}\right) \quad (34)$$

The incomplete gamma function of the second term dominates for short times and we are left with

$$\langle (x_{n\perp}(t) - x_{n\perp}(0))^2 \rangle \sim b^2 t^{3/5} \Gamma_{tb^{4/3}/L^{10/3}} \left(\frac{2}{5}\right) \quad (35)$$

($k_B T, \zeta$, and all constants are set to unity with no loss of generality) The crossover time scale for the perpendicular motion is predicted from this calculation to be

$$\tau_{B\perp} \sim L^{10/3} \quad (36)$$

and can also be described through scaling arguments.

Physically, we expect that a monomer interacts with its neighbors for some time period and then ultimately reaches the wall and bounces off losing 'memory' of its past states. This would imply that the diffusive regime can be completely removed if the confinement width between the two walls is smaller than R_g . The early time behavior will then dominate the monomer motion to a time:

$$\tau_{B\perp}^{3/5} \sim L^2 \Rightarrow \tau_{B\perp} \sim L^{10/3} \quad (37)$$

a time scale which we previously derived through the mode analysis.

Longitudinal Motion To extract the dynamics parallel to the walls, we write down $\langle X_{p\parallel}^2 \rangle_{eq}$ and note that the range of p differs from the perpendicular modes.

$$\begin{aligned} \langle X_{p\parallel}^2 \rangle_{eq} &\sim \frac{N}{p^2} \int_0^N du \cos\left(\frac{p\pi u}{N}\right) \times \\ &\quad \frac{\partial^2 \langle (x_{m\parallel} - x_{n\parallel})^2 \rangle_{eq}}{\partial n \partial m} \\ &\sim \frac{N}{p^2} \int_0^{(L/b)^{4/3}} du \cos\left(\frac{p\pi u}{N}\right) \frac{b^2}{u^{1/2}} \end{aligned}$$

$$\langle (x_{n\parallel}(t) - x_{n\parallel}(0))^2 \rangle \sim \frac{t}{N} + 4 \sum_{p=1}^{\infty} \cos^2\left(\frac{p\pi n}{N}\right) \frac{1}{k_{p\parallel}} \left[1 - \exp\left(-\frac{t}{\tau_{p\parallel}}\right) \right] \quad (39)$$

At these timescales, short compared to $\tau_{p=N/g}$, the summand varies slowly with p and can be approximated as an integral. In the absence of any intrinsic heterogeneities in the chain, we can average over all n and obtain

$$\begin{aligned} &+ \frac{N}{p^2} \int_{(L/b)^{4/3}}^N du \cos\left(\frac{p\pi u}{N}\right) \frac{b^8/3}{L^{2/3}} \\ &\sim \frac{N^{3/2} b^2}{p^{5/2}} F_c \left(\frac{2^{1/2} p^{1/2} L^{2/3}}{N^{1/2} b^{2/3}} \right) \quad (38) \end{aligned}$$

for $p > 0$ and $N \gg 1$. Only the first term in the second line of Eq.(38) is kept because it is comparatively much larger than the second. The functional form is the same as Eq.(31) except that the range of p differs.

The expression for the parallel monomer motion is

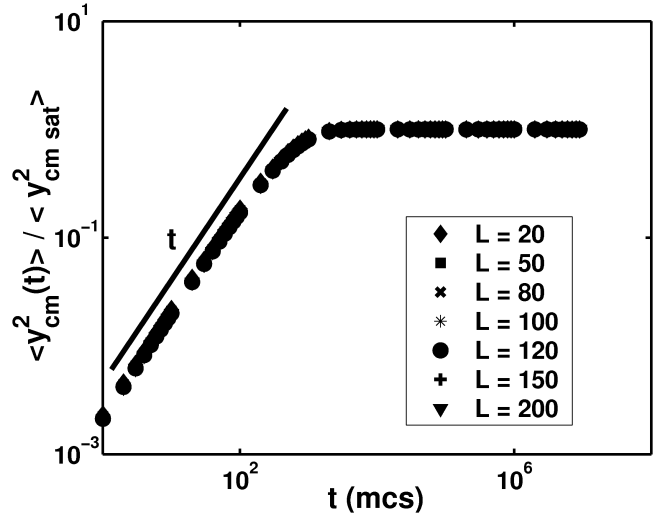


FIG. 10: $N = 500$. Dynamics of the center of mass motion perpendicular to the walls versus time.

The 0th mode is purely diffusive as we expect. To exam-

ine the short time behavior, we again approximate the

sum as an integral and arrive at:

$$\langle (x_{n||}(t) - x_{n||}(0))^2 \rangle \sim \frac{t}{N} + b^{6/5} t^{3/5} \Gamma_{tb^{4/3}/L^{10/3}} \left(\frac{2}{5} \right) + b^{2/3} L^{1/3} \pi^{1/2} t^{1/2} \text{Erf} \left(\frac{t^{1/2} b^{2/3}}{L^{5/3}} \right) \quad (40)$$

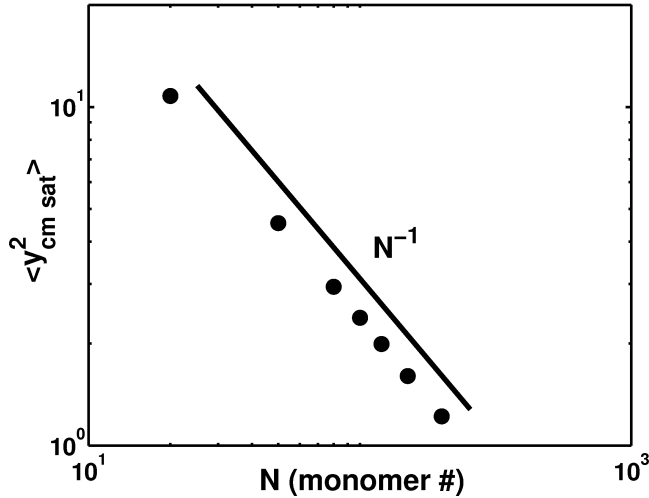


FIG. 11: $L = 20$. Saturation value of the perpendicular motion of the center of mass as function of monomer number.

The system is dominated by the $t^{3/5}$ behavior until the crossover time of $\tau_{B||}$, $\tau_{B||} \sim L^{10/3}$. After $\tau_{B||}$, $t^{1/2}$ becomes the dominant term because the error function in Eq.(40) saturates fairly quickly after $\tau_{B||}$. The $t^{1/2}$ behavior is then cutoff by the 0 th order mode at $\tau_{D||}$ [21].

$$\frac{\tau_{D||}}{N} \sim L^{1/3} \tau_{D||}^{1/2} \Rightarrow \tau_{D||} \sim N^2 L^{2/3} \quad (41)$$

The result that a $t^{1/2}$ interval exists between the $t^{3/5}$ and t behavior can be rationalized based on the blob picture. The number of blobs that make up a polymer in a tube under confinement is N/g . Because of this, we can think of the blobs as being the dominant contributor to the dynamics after $\tau_{B||}$ and before $\tau_{D||}$. However, since the blobs can only move parallel to the walls if neighboring blobs moves, the only other physical mechanism that would lead to a $t^{1/2}$ power law is the compression of the blobs parallel to the walls. Therefore, one interpretation for $\tau_{D||}$ is the longest time associated with the whole polymer compressing[7].

One final point to make is that if we look at the dependence of $\tau_{D||}$ on L , we see that it decreases with decreasing L implying we reach the diffusive regime faster with narrower tubes. The reasoning for this is that the fluctuations perpendicular to the walls are being cut down, but since there is self-avoidance we are forcing the poly-

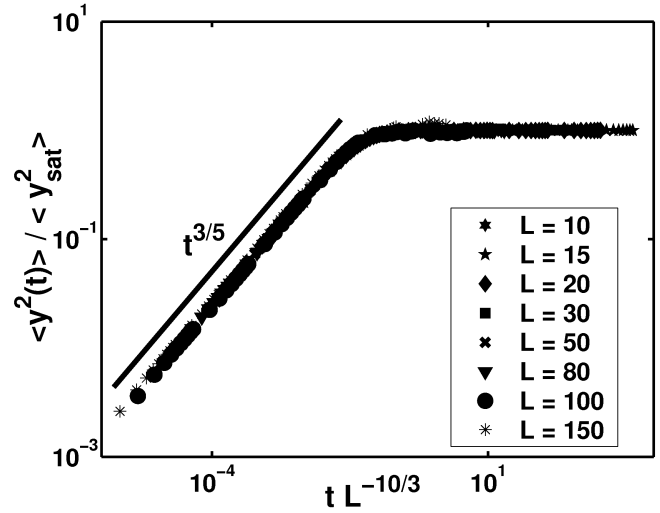


FIG. 12: $N = 500$. Saturation value of the perpendicular motion of a monomer as function of confinement length. Before reaching the walls, the monomer undergoes sub-diffusive behavior predicted by the free polymer scaling arguments. The crossover time can also be predicted from scaling arguments.

mer as a whole more into a rigid rod, which has purely diffusive motion.

End-to-End relaxation Another important quantity in the system is the end-to-end correlation function, the time it takes the polymer to 'forget' about its previous configuration. The long time behavior of this function is[10]

$$C(t) \sim \exp\left(-\frac{t}{\tau_1}\right) \quad (42)$$

where τ_1 is the time scale associated with the longest odd numbered mode. In a tube, we need to look at the perpendicular and parallel components of the relaxation separately. For the perpendicular motion,

$$C_{\perp}(t) \sim \exp\left(-\frac{t}{L^{10/3}}\right) \quad (43)$$

However, for calculating the parallel component, we need to calculate Eq.(30) exactly using Eq.(26) and then take the small p limit[22]. $\langle X_{p||}^2 \rangle_{eq}$ can be approximated as

$$\langle X_{p||}^2 \rangle_{eq} \sim \frac{N^2}{p^4 L^{2/3}} + (O) \frac{1}{p^2} \quad (44)$$

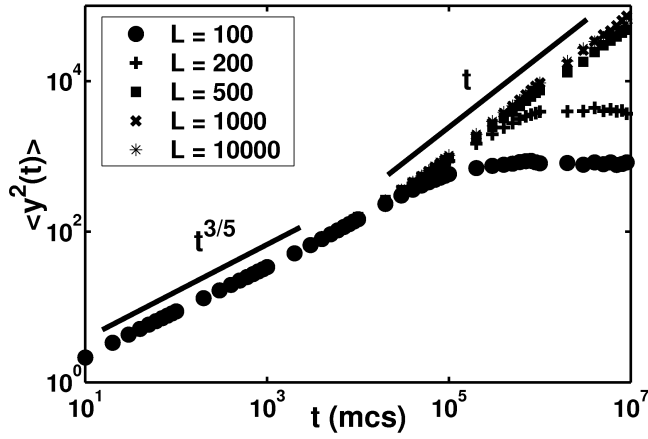


FIG. 13: $N = 500$. Plot of perpendicular monomer motion vs time illustrating the saturation of the perpendicular motion for confinement lengths, $L > R_g$.

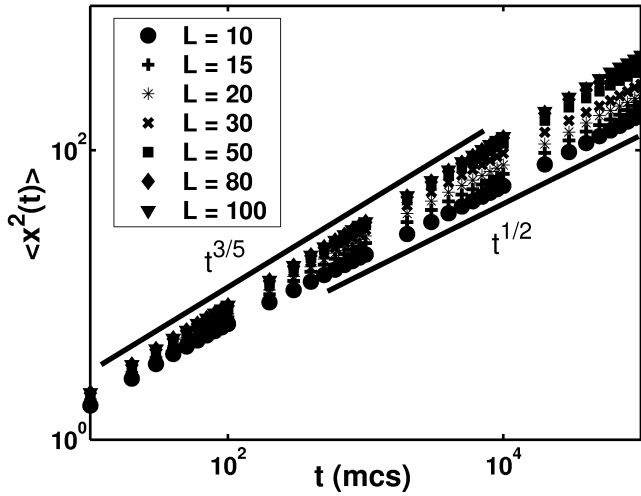


FIG. 14: $N = 500$. Plot of parallel motion vs time showing the change from free chain monomer motion, $t^{3/5}$, to blob dynamics, $t^{1/2}$, by varying the tube width, L . Smaller tube widths lead to blob dynamics occurring at earlier times.

This implies that

$$C_{||}(t) \sim \exp\left(-\frac{tL^{2/3}}{N^3}\right) \quad (45)$$

This result is physically reasonable since the longer the chain or the narrower the tube, the more monomers the ends must go through to exchange positions and decorrelate.

Simulations The simulations serve to support the theoretical results and demonstrate the richness of the dynamics of a single polymer confined to a tube. The results are reproducible and hold very well in the static and dynamical regimes.

For long enough chains, it is possible to reproduce all the monomer-monomer correlation functions. The power laws agree considerably well with the blob picture. We

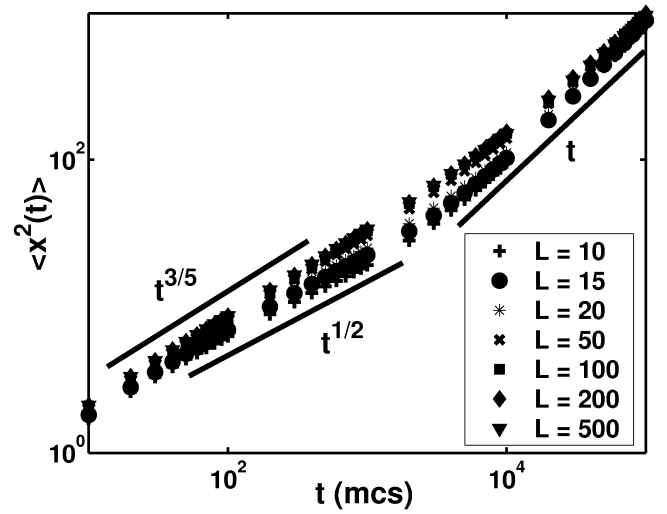


FIG. 15: $N = 50$. In addition to the free monomer diffusion being moved to earlier times, the crossover to purely diffusive behavior also moves to earlier times with a smaller confinement length scale.

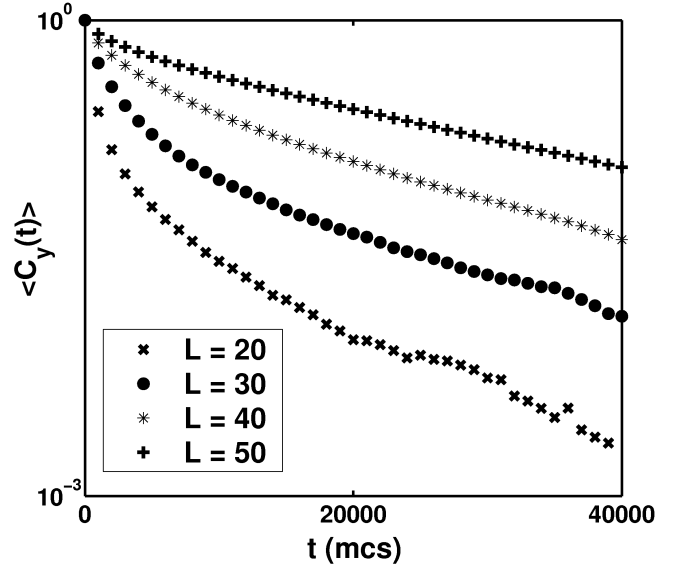


FIG. 16: $N = 200$. Since the tube width is small, there are fewer spots for the end monomers to be which decreases the fluctuations and effectively speeds up the dynamics.

observe some deviations associated with the directions perpendicular to the walls (see Fig.8); however, these are most likely due to hard wall boundaries and have no noticeable effect on the dynamics.

As for the dynamics, the center of mass motion and monomer motion are reproduced reasonably well, though chains longer than $N = 200$ must be simulated in order to recover all three dynamical regimes of the monomer motion clearly. The time scale, $\tau_{B\perp} \sim L^{10/3}$, is in nearly exactly agreement with the theory predictions (see Fig.13). Extracting $\tau_{B||}$, the crossover from $t^{3/5}$ to $t^{1/2}$,

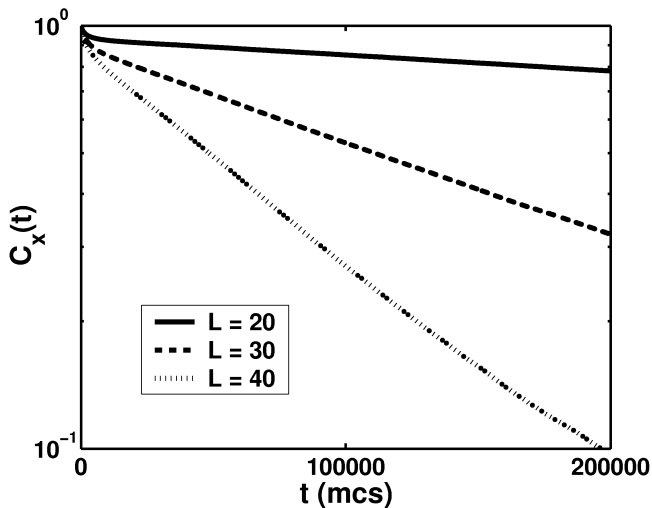


FIG. 17: $N = 200$. Since the polymer is stretched into a tube, the end monomers must travel farther and through more monomers to decorrelate.

from the parallel motion is more difficult. We can make an estimate using Fig.14. The approximate time scale of crossover changes by over two orders of magnitude for a change in tube width of one order of magnitude. For measurements of the end-to-end relaxations, the predicted functional form is in nearly exactly agreement with the blob picture theory and qualitatively the time scales agree with how the longest mode is predicted to behave with a small confinement widths.

Both the end-to-end relaxation and monomer motion depend explicitly on the modes, yet the simulations and theory appear to lead to contradictory pictures particularly in the parallel direction. Shrinking the tube width leads to a smaller $\tau_{D||}$, but a larger τ_1 . Is the dynamics slowing down or speeding up? The contradiction is resolved by recognizing that the slowest modes of the system, those associated with the end-to-end relaxation, are indeed slowing and the faster modes, associated with the monomer motion, are in fact speeding up.

CONCLUSION

We have verified through extensive simulations that the blob picture gives accurate predictions for the size of the chain under hard wall confinement as well as the crossover from 2-D self-avoiding walk statistics to 1-D rod statistics. The slight deviations from the expected scaling arguments are due to one or both of two effects: (a) the lattice spacing associated with the simulation model, (b) the finite length of the polymer. The arguments presented show that the dynamics can be predicted by assuming that the modes of the self-avoiding polymer do not significantly deviate from the modes of an unconfined ideal polymer. The equi-partition theorem then

allows construction of the dynamics from the monomer-monomer correlation function along the polymer.

We expect these results to hold so long as the confinement length scale is less than the radius of gyration of the unconfined polymer[23]. This includes tubes with the ends capped with a distance between the caps being larger than the stretched chain. It is also physically reasonable the each blob has some flexibility associated with it due to the large of amounts of free space in the 2-D SAW that constructs it. Upon assuming that each blob behaves approximately as a spring is another way to acquire a $t^{1/2}$ scaling for the monomer motion[7]; the question as to whether the dynamics are due to compression waves or caging phenomena within a blob is still open and would give more insight into how glasses relax at the single polymer scale or how confined bio-polymers can propagate mechanical stresses from one end to the other.

We can ask all of these questions because of the simplicity of the blob/equi-partition method. It allows for the length and time scales to come out naturally using the equilibrium results; all of this ultimately rests upon using the equilibrium blob picture and incorporating it into the effective dynamics of non-interacting modes.

We acknowledge many useful discussions with Jeremy Schmit and Jane Kondev. This work was supported in part by NSF-DMR 0403997.

-
- [1] J.A. Forrest and K. Dalnoki-Veress, *Adv. Col. and Int. Sci.* **94**, 167 (2001).
 - [2] G.B. McKenna, *J. Phys. iv France* **10**, 246 (2000).
 - [3] J.A. Torres, P.F. Nealey and J.J. de Pablo, *Phys. Rev. Lett.* **85**, 3221 (2000).
 - [4] A.P. Minton, *J. of Bio. Chem.* **276**, 10577 (2001).
 - [5] X.S. Xie et. al., *Science* **302**, 262 (2003).
 - [6] M. Daoud and J.P. Cotton, *J. Phys. (Paris)* **43**, 531 (1982).
 - [7] F. Brochard and P.G. de Gennes, *J. Chem. Phys.* **67**, 52 (1977).
 - [8] T. Sakaue and E. Raphael, *Macromolecules* **39**, 2621 (2006).
 - [9] K. Kremer and I. Carmesin, *Macromolecules* **21**, 2819 (1988).
 - [10] M. Doi, *Introduction to Polymer Physics* (Oxford University Press, 1995).
 - [11] A. Di Cecca and J.J. Freire, *Macromolecules* **35**, 2851 (2002).
 - [12] C.-M. Chen and Y.-A. Fwu, *Phys. Rev. E* **63**, 011506 (2000).
 - [13] N. Gilra, A.Z. Panagiotopoulos, and C. Cohen, *J. Chem. Phys.* **115**, 1100 (2001).
 - [14] R. Azuma and H. Takayama, *cond-mat/9906021* (Jun 1999).

- [15] P.J. Flory, J. Chem. Phys. **17**, 303 (1948).
- [16] M. Doi and S.F. Edwards, *The Theory of Polymer Dynamics* (Oxford University Press, 1988).
- [17] J.L. Cardy, J. Phys. A **16**, 3617 (1983).
- [18] P.G. de Gennes, *Scaling Concepts in Polymer Physics* (Cornell University Press, 1979).
- [19] P. Pincus, Macromolecules **9**, 386 (1976).
- [20] D. Molin, A. Barbieri, and D. Leporini, J. Phys.:Cond. Mat. **18**, 7543 (2006).
- [21] P.G. de Gennes, J. Chem. Phys. **55**, 572 (1971).
- [22] Y.-J. Sheng and M.-C. Wang, J. Chem. Phys. **114**, 4724 (2001).
- [23] K. Kremer and K. Binder, J. Chem. Phys. **81**, 6381 (1984).